doi:10.1111/evo.12781

Virulence evolution at the front line of spreading epidemics

Quentin Griette,[1,2,3] Gaël Raoul,[2,4] and Sylvain Gandon[2]

[1]*Département de Mathématiques, Faculté des Sciences, Université de Montpellier, Place Eugène Bataillon, Montpellier, France*

[2]*CEFE - UMR 5175, campus CNRS, 1919 route de Mende, 34293 Montpellier, France*

[3]*E-mail: quentin.griette@univ-montp2.fr*

[4]*CMAP - UMR 7641, École Polytechnique, CNRS, Route de Saclay, 91128 Palaiseau Cedex, France*

Received May 19, 2015
Accepted September 14, 2015

Understanding and predicting the spatial spread of emerging pathogens is a major challenge for the public health management of infectious diseases. Theoretical epidemiology shows that the speed of an epidemic is governed by the life-history characteristics of the pathogen and its ability to disperse. Rapid evolution of these traits during the invasion may thus affect the speed of epidemics. Here we study the influence of virulence evolution on the spatial spread of an epidemic. At the edge of the invasion front, we show that more virulent and transmissible genotypes are expected to win the competition with other pathogens. Behind the front line, however, more prudent exploitation strategies outcompete virulent pathogens. Crucially, even when the presence of the virulent mutant is limited to the edge of the front, the invasion speed can be dramatically altered by pathogen evolution. We support our analysis with individual-based simulations and we discuss the additional effects of demographic stochasticity taking place at the front line on virulence evolution. We confirm that an increase of virulence can occur at the front, but only if the carrying capacity of the invading pathogen is large enough. These results are discussed in the light of recent empirical studies examining virulence evolution at the edge of spreading epidemics.

KEY WORDS: **Epidemiology, evolution, space, stochasticity, virulence.**

The emergence of infectious diseases is an ever-increasing source of concern for human health, agriculture, and wildlife conservation. Understanding the epidemiological dynamics of pathogen populations may help limit the potentially devastating consequences of epidemics for animal and plant species. For instance, it is particularly important to understand which factors govern the speed of epidemics to predict and potentially prevent the spatial spread of pathogens. Historical reports allow estimating the speed of various epidemics such as the Black Death in the 14th century (320–650 km/year) or rabies in Europe in the last century (30–60 km/year) (Shigesada and Kawasaki 1997). More recently, several studies indicate that the speed of epidemics is not constant but can accelerate with time (Mundt et al. 2009). Even more complex spatiotemporal patterns have been described in measles spreading in heterogeneous host populations (Grenfell et al. 2001). Is it possible to understand what governs this diversity of invasion patterns from one disease to another?

Determining the speed of biological invasions has attracted a lot of attention from theoretical biologists (Fisher 1937; Kolmogorov et al. 1937; Skellam 1951). Under the simplifying assumption that the environment is homogeneous and that the kernel of dispersal is normally distributed, diffusion models can be used to predict the asymptotic speed of the spatial spread of the population (Fisher 1937; Kot et al. 1996; Shigesada and Kawasaki 1997). Typically, the population spreads as a traveling wave with a speed equal to $2\sqrt{\sigma r}$, where r is the exponential growth rate of the population at low density and σ is the diffusion coefficient that measures how quickly the organisms disperse (Shigesada and Kawasaki 1997). Relaxing the underlying assumptions of this model may alter quantitatively the speed of the traveling wave. For instance, adding spatial and/or temporal heterogeneity in the environment may speed up or slow down (depending on which parameter is affected by the environment) the invasion (Shigesada and Kawasaki 1997; Seo and Lutscher 2011; Eller and Schreiber

EVOLUTION
INTERNATIONAL JOURNAL OF ORGANIC EVOLUTION

2012). Modifying the shape of the dispersal distribution may have even more dramatic consequences on the invasion dynamics. In particular, fat-tailed kernels of dispersal can generate accelerating invasions rather than constant-speed traveling waves (Kot et al. 1996; Shigesada and Kawasaki 1997).

Previous studies have mostly focused on the spatial dynamics of invasions under the assumption that evolutionary dynamics could be neglected because it is a much slower process (Perkins 2012). There is overwhelming evidence, however, that evolution is often very rapid during invasions (Perkins et al. 2013). In particular, spatial sorting drives dispersal evolution at the invasion front and may result in the accumulation of individuals with extreme dispersal abilities at its edge. This spatial sorting of phenotypes (Shine et al. 2011) may also act on other phenotypic traits. Indeed, the edge of the front is characterized by low-density dependence and may select for higher growth rates (Phillips 2009; Burton et al. 2010). Because selection for higher σ and higher r is expected to affect propagation speed, rapid evolution may be another factor that could generate accelerating invasions (Perkins 2012; Perkins et al. 2013). Pathogens are likely to exhibit rapid evolution during an epidemic. Viral populations, in particular, are often characterized by large population sizes and large mutation rates that may fuel the genetic variability of pathogen populations (Holmes 2009). This genetic variability implies that epidemiological and evolutionary processes occur simultaneously. Evolutionary epidemiology theory tracks the transient dynamics of pathogens during epidemics taking place in well-mixed environments (Day and Proulx 2004; Day and Gandon 2007; Berngruber et al. 2013). The influence of spatial structure on the ultimate evolution of virulence has been examined in several earlier studies (Boots et al. 2004; Lion and Boots 2010; Lion and Gandon 2015). But most of those studies focused on the long-term evolution of the pathogen after it has reached an endemic equilibrium. Wei and Krone (2005), in contrast, studied the emergence of mutant pathogens in phage epidemics spreading in a lawn of susceptible bacteria. They pointed out that the invasion success of a mutant pathogen depends on the life-history traits of the mutant and the location of the mutant relative to the front of the epidemic. More recently, Osnas et al. (2015) studied the interplay between the pathogen's virulence and its influence on the host's ability to disperse. In their model, the wave of the epidemic can be invaded by a low virulence strain, which diffuses faster, and is followed by an intermediate virulence strain before reaching the evolutionary equilibrium. Here we extend previous studies and follow epidemiology and evolution during the spatial spread of an epidemic. We develop a model based on reaction–diffusion equations to understand virulence evolution and its impact on the speed of an epidemic taking place in a homogeneous host population. This deterministic model shows how mutation can affect the epidemiological dynamics and speed up the spatial spread of a pathogen. We explore the robustness of these conclusions in various epidemiological scenarios under a broad range of pathogen life cycles. Finally, we confront these analytical results with individual-based simulations and explore the impact of demographic stochasticity on invasion dynamics.

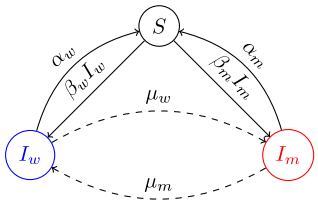

Figure 1. Schematic representation of the pathogen life cycle. Arrows represent the transitions between states. The label indicate the rates at which those transitions occur.

Model

EPIDEMIOLOGY AND EVOLUTION

We use a classical epidemiological model where the host can either be susceptible or infected. We assume that two pathogen genotypes are circulating in the host population: a wild-type genotype (w) and a mutant genotype (m). Coinfections with the two genotypes are not allowed. Each genotype i ($i \in \{w, m\}$) is characterized by two specific life-history traits. First, β_i is the rate at which transmission occurs between infected and susceptible hosts after a contact. Second, α_i is the mortality rate of infected hosts. Mutation may occur between these two genotypes and μ_i stands for the rate of mutation from genotype i to the other genotype (see Fig. 1). The transmission of the pathogen is assumed to be local (infected hosts can only infect susceptible hosts at the same spatial location) but both susceptible and infected hosts are allowed to diffuse in one dimension with a fixed rate σ. In other words, we neglect the influence the pathogen may have on the mobility of its hosts. The densities of the different types of host at location x and time t are noted $S(x,t)$ (susceptible hosts) and $I_i(x,t)$ (infected hosts with genotype i). For the sake of simplicity, we assume that dead hosts are immediately replaced by new susceptible hosts. Consequently, the total host population size is assumed to remain constant and equal to $N = S(x,t) + I_w(x,t) + I_m(x,t)$. Our model can thus be written as a set of reaction–diffusion equations (for readability, we drop the time and space dependence notation in the following):

$$\begin{cases} \dfrac{\partial I_w}{\partial t} = \sigma \dfrac{\partial^2 I_w}{\partial x^2} + r_w I_w \left(1 - \dfrac{I_w + I_m}{K_w}\right) + \mu_m I_m - \mu_w I_w \\ \dfrac{\partial I_m}{\partial t} = \sigma \dfrac{\partial^2 I_m}{\partial x^2} + r_m I_m \left(1 - \dfrac{I_w + I_m}{K_m}\right) + \mu_w I_w - \mu_m I_m \end{cases} \quad (1)$$

with $r_i = \beta_i - \alpha_i$ and $K_i = N(1 - \frac{\alpha_i}{\beta_i}) = N(1 - \frac{1}{R_{0,i}})$ (see derivation in Section 1 of the Supporting Information). In the following,

we focus on situations where $r_i > 0$, meaning that both pathogens have the ability of producing an epidemic. With these assumptions, r_i can be interpreted as a growth rate and K_i as a carrying capacity for each respective strain. In the Supporting Information (Section 10), we provide more information concerning the link between the epidemiological parameters α and β, and the ecological ones r and K. Note that $R_{0,i} = \frac{\beta_i}{\alpha_i}$ measures the basic reproductive ratio of genotype i. It can be shown that if we assume $r_i > r_j$ and $K_i > K_j$ strain, j is outcompeted by strain i throughout the habitat.

In addition we assume that $r_m > r_w$ and $K_w > K_m$. In other words, we are considering a situation where a wild-type genotype can give rise to a virulent genotype by mutation. Increased virulence is detrimental to pathogen fitness (notice that $K_m < K_w$ is equivalent to $R_{0,m} < R_{0,w}$) but we assume that this mutation has a pleiotropic effect and is associated with an increased transmission rate. Our hypothesis can be reformulated in terms of epidemiological parameters : given a wild-type phenotype (β_w, α_w), an admissible mutant has a phenotype (β_m, α_m) satisfying the constraint : $\beta_m < \alpha_m R_{0,w}$ and $\beta_m > (\beta_w - \alpha_w) + \alpha_m$. This is a classical scenario considered to understand the evolution of pathogen virulence (Frank 1996; Alizon et al. 2009). The originality of the present model is to study this joint epidemiological and evolutionary dynamics in a spatially explicit context.

Results

EPIDEMIC SPEED

Numerical solutions of (1) have a distinctive shape represented in Figure 2 that proves to be very robust under a broad range of parameter values. The mutant genotype is always present at the front because it has a higher instantaneous rate of growth r_m. Away from the front, however, the wild-type genotype outcompetes the mutant genotype because it has a higher carrying capacity K_w (i.e., the wild type has a higher basic reproductive ratio $R_{0,w}$). Using a linear approximation near the edge of the front, we obtain an analytical expression for the speed (presented in (2) ; see also Section 2 of the Supporting Information) of the traveling waves associated with equation (1).

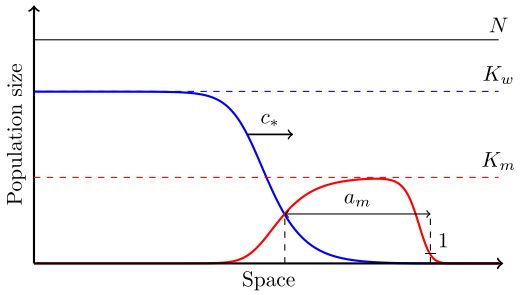

Figure 2. Shape of the stationary front of the spreading epidemic. The epidemic moves at a constant speed c^*. The mutant genotype (in red) is prevalent at the edge of the front and reaches a maximal density of K_m. Behind the front, the wild-type genotype (in blue) takes over and reaches a higher density K_w. The size of the area where the mutant is more abundant that the wild type is called the mutant's range, a_m.

$$c^* = \sqrt{2\sigma\left(r_w + r_m - (\mu_w + \mu_m) + \sqrt{(r_m - r_w)^2 + 2(r_w - r_m)(\mu_m - \mu_w) + (\mu_w + \mu_m)^2}\right)}. \quad (2)$$

When both μ_w and μ_m are assumed to be small, the speed of the epidemic reduces to

$$c^* = c_m - \kappa(\mu_w, \mu_m) + o(\mu_w, \mu_m), \quad (3)$$

where $c_m = 2\sqrt{\sigma r_m}$ is the deterministic speed of the mutant alone, and κ is a linear function representing the mutation load on the speed:

$$\kappa(\mu_w, \mu_m) = \sqrt{\frac{\sigma}{r_m}}(3\mu_m - \mu_w).$$

In other words, the spatial dynamics of the whole epidemic is mainly driven by the mutant genotype. In particular, it is driven by its instantaneous growth rate r_m. When an epidemic starts from a population composed only of wild type, it will at first behave like the wild type and experience a transitory phase before reaching the behavior of a traveling wave. We did a brief presentation of these transitory dynamics in Section 3 of the Supporting Information.

MUTANT'S RANGE

To better characterize the front of the epidemic, we derive an approximation for the size of the area a_m where the mutant is abundant (Fig. 2). This approximation is based on a set of simplifying assumptions to capture the main steps of the competition going on during the invasion. First, we assume that one mutant is introduced and grows exponentially to carrying capacity with rate r_m. When the mutant reaches its carrying capacity K_m, the wild type is introduced at rate μ_m from the population of mutants and grows at rate r_w until its density becomes higher than K_m (see Section 4 of the Supporting Information for the derivation).

The approximation for the mutant's range is defined as the spatial distance between the tip of the front and the point where the density of the wild type becomes higher than the mutant's:

$$a_m \approx 2\sqrt{\frac{\sigma}{r_m}}\log(K_m) - \frac{2\sqrt{\sigma r_m}}{\left(1 - \frac{K_m}{K_w}\right)r_w}\log\mu_m. \quad (4)$$

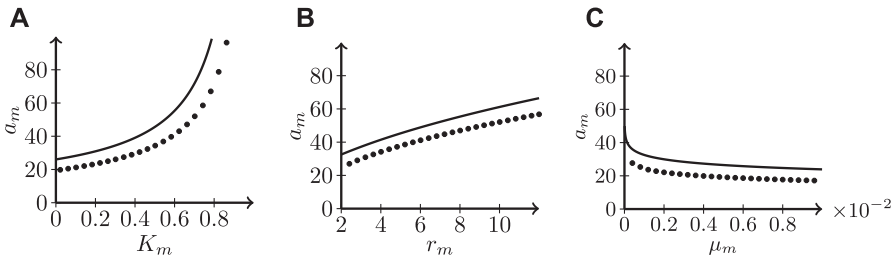

Figure 3. Effects of K_m, r_m, and μ_m on the size of the mutant's range a_m in (A), (B), and (C), respectively. The full lines present the approximation given in (4). The dots present the mutant's range obtained from numerical simulations at time $t = 500$.

This expression captures the effect of several parameters. In particular, the mutant's range increases with r_m and K_m, which measure the competitive ability of the mutant at the tip of the front and behind the front, respectively. As expected the mutant's range decreases when the influx μ_m of wild-type genotypes increases. Figure 3 shows that this approximation agrees well with the mutant's range derived from numerical solutions of equation (4).

MUTATION-SELECTION EQUILIBRIUM BEHIND THE FRONT

The above results characterize the speed and the shape of the front. Behind the front, the wild-type genotype outcompetes the mutant but mutation μ_w can reintroduce the mutant in the pathogen population. The equilibrium density of the mutant results from the balance between mutation and selection. Under the assumptions that mutation rates remain low relative to the growth rates and that the pathogen population is equal to K_w, we recover a classical result from population genetics (Crow and Kimura 1970) on the equilibrium frequency (see Section 5 of the Supporting Information):

$$p_{eq} \approx \frac{\mu_w}{s}, \tag{5}$$

where s measures the selection against the mutant at the endemic equilibrium (for more information about s, see Section 5 in the Supporting Information). It is worth noting that the mutation load behind the front is mainly governed by the mutation rate μ_w, whereas the mutation load on the speed of the epidemic is mainly driven by μ_m (see (3)). This is because selection varies between the edge of the front (where the mutant is selected for) and behind the front (where the mutant is selected against).

ALTERNATIVE EPIDEMIOLOGICAL MODELS

Our model relies on the assumption that dead hosts are immediately replaced by susceptible ones and that infected hosts cannot recover from the infection. We relaxed these assumptions and analyzed the epidemiology and evolution under alternative epidemiological models. First, we examined a situation where there is no host reproduction (see details in Section 6.1 of the Supporting Information). This model may be relevant to describe the spatial spread of a bacteriophage on a bacterial lawn (Wei and Krone 2005). When lytic bacteriophages spread, the burst of bacterial cells release new virions but rapidly exhausts the resource (i.e., host density drops) behind the front. Yet, when a virulent strain is allowed to appear by mutation, we recover the profile described above (Fig. S2). We also examined a situation where the infected hosts can recover and become immune to the infection (see details in Section 6.2 of the Supporting Information). Here, again, we recover the same qualitative result (Fig. S3) where the mutant is at the edge of the front and it is replaced by the wild type. The main difference between these two scenarios and the original model (1) is the drop in the density of the wild type behind the front. Note that this drop may be characterized in the second scenario by damped oscillations when recovery rates are large (Shigesada and Kawasaki 1997). These alternative models do not alter qualitatively our results because these modifications of pathogen's life cycle do not affect processes going on at the edge of the front. In particular, the formula for the speed remains valid. However, the specific structure of equation (1) is only valid as a first-order approximation near the edge of the front in those cases. This is true for the formula of K, which may no longer correspond to the carrying capacity in the back of the front. Other modifications of the life cycle can have a more profound impact on evolutionary dynamics. For instance Osnas et al. (2015) assumed that infected hosts have a lower tendency to disperse. This selects for lower virulence at the front of the epidemic. In all those scenarios, however, the parasite strain taking over at the edge of the front are the ones characterized with the fastest rate of spread of the epidemic wave.

STOCHASTIC SIMULATIONS

The above results are derived from a fully deterministic model. We explored the effect of stochasticity using an individual-based model that takes into account that the number N of hosts per site is finite and h measures the spatial distance between sites. As above, hosts can be in three states : susceptible, infected by a wild-type pathogen, or infected by a mutant pathogen. The individual transitions between these states are described by a list of random

events (transmission, mutation, death ; see Fig. 1 and Section 7 of the Supporting Information for a detailed description). This stochastic model converges to the above deterministic model (1) when N is assumed to be very large.

To catch the front dynamics, we performed simulations with our individual-based model and measured the average speed on a long period after the influence of the initial condition is lost. These simulations show that the asymptotic speed of the epidemic depends on the number of individuals per unit of space. A lower host population size reduces the speed of the front. This effect is due to the stochasticity occurring at the edge of the front. In contrast with the deterministic model, the density at the front cannot fall below $1/N$ (it takes at least one infected host over the N possible hosts to create a front). This discreteness affects the shape of the front and, consequently, the speed of the traveling wave. Following Brunet and Derrida (1997) and Mueller et al. (2011), we obtained an approximation that captures the effect of finite population size on the speed of the front (see details in Section 8 of the Supporting Information):

$$c_i^{stoch} \approx c_i - \sqrt{\sigma r_i}\left(\frac{\pi}{\log\left(\frac{K_i}{h}\right)}\right)^2.$$

This estimate matches the qualitative asymptotic behavior of the speed and becomes increasingly accurate as h goes to zero (recall that h measures the distance between sites and π is the mathematical constant). Figure S4 shows that the match between this approximation and the simulation is not very good when population size gets very low. Yet the approximation captures the qualitative effect of finite population size. In particular, we see that the speed of the mutant is more affected by finite population size. There is a critical population size below which the front of the mutant is slower than the front of the wild type. In that situation the mutant cannot invade and the epidemic is driven by the wild-type genotype. When population size increases there is a region where the front oscillates between the wild type and the mutant. When the mutant manages to be at the front, the speed increases (see Fig. S4) but the mutant can get lost stochastically due to genetic drift. For larger population sizes, the mutant can remain at the front for longer periods of time and the speed of the traveling wave increases. As expected, for infinitely large host populations, the speed of the epidemic converges to c^*.

We also developed a two-dimensional version of our stochastic simulation model. Figure 4 presents the results under different scenarios. This figure illustrates the impact of the initial condition and the strength of selection on (1) the genotypic diversity in a growing epidemic, (2) the spatial distribution of this diversity, and (3) the speed of the epidemic. In particular, if the introduction of virulent genotypes is conditional on a mutation event, the mutant genotype will emerge later than if genetic diversity is present at the onset of the epidemic. This affects the frequency of mutants for all the different values of selection intensity. When selection is strong, the late arrival of the mutant has also a direct impact on the speed of the front and, consequently, on the overall size of the epidemic (compare the radius of the infected population in D and E, see also Fig. S1). The strength of selection also affects the distribution of genetic diversity. In the absence of selection, we recover the patterns described by Hallatschek and Nelson (2009). The interplay between the spatial spread of the epidemic and the stochasticity occurring at the front generates characteristic quadrants that are either dominated by one genotype or the other. When there is some selection, we can recover these quadrants but their shape is altered by competitive interactions (Fig. 4). At the front line of the epidemic, the mutant is a better colonizer and spreads faster. Behind the front, the wild-type genotype is more competitive and tends to replace the mutant genotype. When selection is strong, the mutant only appears at the front and the core of the epidemic is dominated by wild-type genotypes.

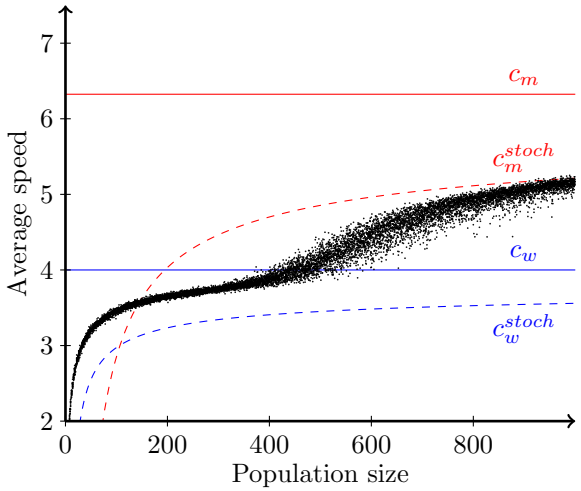

Figure 4. Effect of host population size *N* on the average speed of the stochastic epidemic. Hundred simulations were done for each value of *N* and each dot represents the average epidemic speed for a single simulation, taken between time *t* = 200 and *t* = 1000.

Discussion

Improving our ability to control infectious diseases requires a better understanding of both the epidemiology and the evolution of pathogens. Our theoretical understanding of virulence evolution is often based on the assumption that evolution occurs on a much slower time scale than epidemiological dynamics. Yet, epidemiological and evolutionary time scales overlap in many pathogens because large amount of genetic variation fuel the rate of adaptation (Holmes 2009). In these situations, evolutionary epidemiology theory provides a way to describe accurately the

pathogen dynamics during an epidemic and shows how epidemiology can feed back on evolution (Lenski and May 1994; Frank 1996; Day and Gandon 2007; Bull and Ebert 2008; Gandon and Day 2009; Bolker et al. 2010; Berngruber et al. 2013). During the early stage of the epidemic more virulent and transmissible strains are favored because susceptible hosts are abundant. Later on, the density of susceptible hosts is reduced and can reverse the selection on virulence and transmission. Here we extend this theoretical framework to account for the spatial spread during epidemics. We show that more virulent genotypes are favored at the front line of the epidemic and counterselected behind the front. This heterogeneity of selection is akin to the classical distinction between r and K selection during an invasion (MacArthur and Wilson 1967; Pianka 1970, 1972). This spatially and temporally variable selection has the ability to maintain diversity. Interestingly, the speed of the whole epidemic (both the wild type and the mutant genotypes) is mainly governed by the presence of the virulent mutant at the front. Hence, even though the presence of the mutant may be limited to a very small range behind the front (in particular, when K_m is small), the epidemic may spread much faster when mutation is allowed because the epidemic is pulled by the spread of the virulent mutant at the front. In other words, pathogen evolution feeds back on epidemiological dynamics by speeding up the spread of the pathogen's traveling wave. This result points out a possible flaw in our ability to infer pathogen's growth rate from the speed of the epidemic. If the genotypes at the front are distinct from the ones spreading behind the front, the speed may only help characterize the growth rate of a fraction of the pathogen population. Our analysis is limited to a situation with only two genotypes (the wild type and the mutant). It would be interesting to allow for a continuum of genotypes. We believe that this scenario would yield similar outcomes: we expect that at the front line, genotypes maximizing the Malthusian fitness would be selected, while behind it, genotypes with higher carrying capacity would dominate. Hence, we would retrieve the dichotomy assumed in the present model and observe a continuous phenotypic gradient between these two extremes (Perkins 2012; Alfaro et al. 2013).

Empirical evidence supporting the above theoretical predictions requires an intense sampling effort across a moving epidemic. An interesting biological system is the virus dynamics observed in honeybee colonies along a new expansion front (Mondet et al. 2014). Virus transmission is often tightly linked with the presence of the parasitic mite *Varroa destructor*. In particular, the acute bee paralysis virus (ABPV) and the deformed wing virus (DWV) are actively transmitted by *Varroa*. Interestingly, the virulence of ABPV is much higher than the virulence of DWV. In line with our theoretical predictions, the ABPV is often found at the edge of the front and is rapidly outcompeted by the DWV (Mondet et al. 2014). This pattern may be driven by selection for a r-strategy (APBPV) at the front line and selection for a K-strategy (DWV) behind the front. ABPV and DWV, however, belong to different species complex and mutation does not seem to provide the ability to jump between these different virus forms. This pattern is akin to ecological successions (Shigesada and Kawasaki 1997) but is not driven by mutation and selection. Further confirmation of the importance of mutation and evolution was obtained with the fungal pathogen *Batrachochytrium dendrobatidis* (*Bd*) in common garden experiments. This pathogenic fungus is known to be the main driver of the recent decline of many amphibian populations around the world (Berger et al. 1998; Voyles et al. 2009). The wave-like spread of this pathogen in Central America has been well monitored (James et al. 2009). Besides, genetic evidence suggests the ability of mutations to generate a new hypervirulent strain of *Bd* (James et al. 2009; Farrer et al. 2011; Velo-Antòn et al. 2012). This biological system has thus all the key elements of our model (spatial spread and mutation). Interestingly, Phillips and Puschendorf (2013) discuss the possibility that *Bd* virulence may have increased at the front line of the epidemic. This evidence, however, is indirect because it is based on the rate of decline of the host population after the contact with *Bd* and many other abiotic factors may be involved. It would be particularly interesting to confirm this trend in a common garden experiments. Such an experiment was carried out to monitor the evolution of the nematode lungworm (*Rhabdias marina*), a parasite of the invasive cane toads (*Rhinella marina*) in Australia (Kelehear et al. 2012). Nematodes from the edge of the invasion exhibited very distinct life-history traits (larger eggs, larger free-living larvae, larger infective larvae, and reduced age at maturity). These results support the general prediction that pathogens may rapidly evolve colonizer syndromes. Whether this evolution leads to higher virulence and faster epidemic spread is unclear in this particular system where the pathogen follows the spread of its host with a lag of several years. What limits the speed is more the availability of the host than the intrinsic epidemic speed. It would be interesting to expand the analysis of our model to a scenario where the speed of the host is lower than the speed of the pathogen. In this case, the pathogen present at the edge of the front experiences a relatively low density of hosts and this may select for lower virulence strategies (see also discussion in Shine et al. 2011, where the pathogen may affect the speed of the host invasion).

Experimental evolution may also provide ways to test our predictions. Complex life-history trade-offs may emerge in bacteriophages because the instantaneous rate of growth of lytic phages is governed by a limited number of traits (adsorption rate, lysis time, burst size, Bull 2006). Besides, the adsorption rate is also acting on the diffusion rate of the phage (Gallet et al. 2011). Under these conditions spatial structure is expected to select for lower infectivity and virulence (Boot and Sasaki 1999; Haraguchi

and Sasaki 2000; Lion and Boots 2010; Lion and Gandon 2015). Several experiments have confirmed that spatial structure can select for less-aggressive pathogen strategies in bacteriophages (Eshelman et al. 2010; Roychoudhury et al. 2014; Berngruber et al. 2015). But those studies never focused on the spatial distribution of the different types of strains across an epidemic. Yin (1993), however, realized a very nice experiment with phage T7 where evolution was monitored during the spatial spread of the virus. Unlike other lytic phages, T7 has the ability to form plaques that grow indefinitely large on agar plates (Yin 1991). Monitoring the growth of the plaque allowed to determine the speed of the epidemic and sampling across the plaque allowed to detect the emergence and the fixation of phage mutants at the edge of the front. Those mutants were characterized with higher fitness in both liquid and spatially structured environments (Yin 1993) and it is unclear if this particular system matches the underlying assumptions of our model (i.e., $r_m > r_w$ and $K_w > K_m$). But further work using Yin's experimental approach and detailed phenotypic characterization of the strains across an epidemic could help test some of our theoretical predictions.

The analysis of the stochastic version of our model reveals three effects of finite host population size. First, finite population size has a direct effect on the speed of a monomorphic population. Smaller population sizes reduce the speed because they induce a cutoff in the tail of the distribution at the forefront of the epidemic (Brunet and Derrida 1997; Snyder 2003). Second, the magnitude of this effect depends on the life-history traits of the pathogen: the effect is stronger on the virulent genotype than on the wild type because stochasticity is driven by the population size of each genotype. The lower carrying capacity of the mutant makes it more susceptible to the effect of stochasticity mediated by total host population size N. Hence, the speed of the virulent mutant may become lower than the wild type. Third, stochasticity may result in the extinction of the mutant at the edge of the front. This is related to the effect of the basic reproductive ratio on the probability of emergence (Gandon et al. 2013). The probability of emergence (i.e., the probability of nonextinction) is driven by the basic reproductive ratio and thus by K_i. When mutation is allowed, small population sizes may thus prevent the establishment of the virulent mutant at the edge of the front because $K_w > K_m$. This effect may further decrease the speed of the epidemic. These multiple effects may provide a particularly efficient way to slow down an epidemic. Lowering the availability of some hosts by prophylactic intervention is expected to reduce the local transmission rate (and thus both r_i and K_i) but it may also allow these stochastic effects to play in. It is interesting to discuss the effects of stochasticity in the light of recent population genetics theory on gene surfing (Hallatschek and Nelson 2007, 2009; Peischl et al. 2013). Gene surfing is mostly studied in scenarios describing the establishment of neutral or deleterious mutations during an invasion. In our model, selection is not homogeneous in space and time because epidemiology feeds back on the relative fitness of the mutant via the availability of susceptible hosts. This type of selection, when it is strong, can dramatically alter the spatial distribution of genotypes (Fig. 5). Epidemiological phylodynamics may provide a way to test some of our predictions. For instance, Biek et al. (2007) analyzed the spatial spread of rabies virus in North American racoons. Their data were consistent with gene surfing models where different strains occupy different sectors of the spreading disk of the epidemic. More elaborate techniques have also been used to estimate pathogen life-history parameters

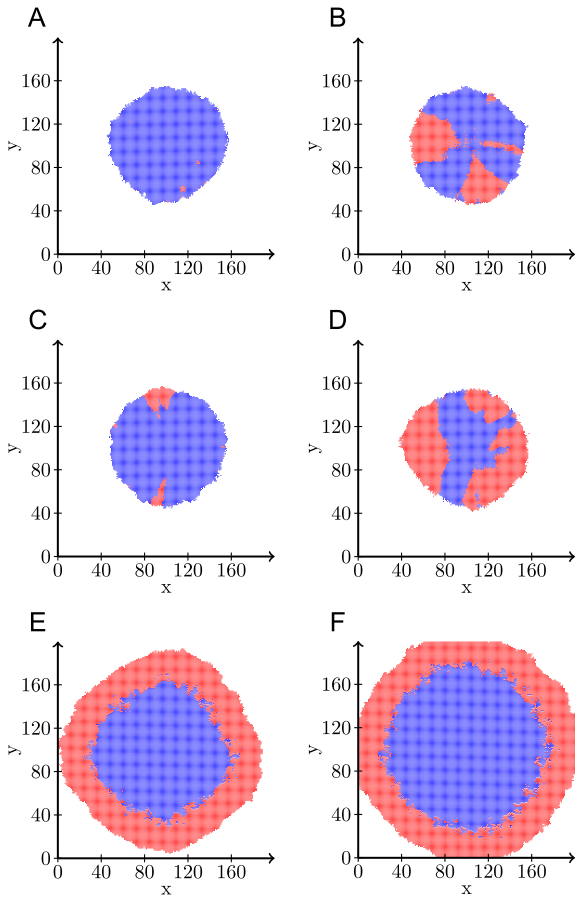

Figure 5. Stochastic simulations of the spread of an epidemic in two dimensions (*x* and *y*). At the beginning of the simulation, the pathogen population starts as a disk of radius 6.3 cells. In (A), (C), and (E), the simulation starts from an initial condition where only the wild type is present. In (B), (D), and (F), the simulation starts from a mixed pathogen population where the wild type and the mutant are equally frequent. In the first row (A and B), the wild type and the mutant have the same parameter values (neutral selection scenario). In the second row (C and D), the mutant is slightly more virulent than the wild type (weak selection scenario). In the third row, the mutant is very different from the wild type (strong selection scenario). The actual parameters we used can be found in the Supporting Information (Section 12).

(Pybus et al. 2012). These new theoretical developments and the availability of more genetic information may provide a way to infer the most likely epidemiological scenario from the examination of spatial distributions of genetic diversity (Fig. 5).

It is worth pointing out that our model could also be used to better understand coevolution between virulence and antigenic drift occurring in influenza virus in the absence of geographic spatial structure. Influenza evolution is often described as a traveling wave in phenotypic space where the strains at the edge of the front are the ones that are not recognized by the host immune system (Gog and Grenfell 2002; Boni et al. 2006). In those models the diffusion coefficient in phenotypic space refers to the mutation occurring between strains with different antigens. New strains have access to a higher density of susceptible hosts and this could affect selection acting on other life-history traits (transmission and virulence). Our results show that one could expect pathogen virulence to be higher at the edge of this front, and to decrease in older strains because of herd immunity. Yet, to explicitly model the joint evolution of antigenic drift and virulence, it is necessary to take into account the genetic linkage between those traits (Day and Gandon 2012).

Evolutionary theory has shown that the adaptation of invasive species may involve a multiplicity of life-history traits. In particular, the diffusion parameter σ is likely to be under strong positive selection at the edge of the front (Shine et al. 2011). In our model the diffusion rate is under the control of the host. Other life cycles with free-living stages may be considered, where this trait could be under the control of the pathogen. Further theoretical developments are required to analyze scenarios where multiple other traits may coevolve with virulence and transmission (Burton et al. 2010; Perkins et al. 2013; Osnas et al. 2015). Besides, it would be particularly relevant to consider the possibility that pathogens spread in a heterogeneous host habitat (e.g., multiple host environments). The impact of various forms of heterogeneity on the spread of invasive species has been studied in monomorphic populations (Shigesada and Kawasaki 1997). Allowing mutation would fuel pathogen evolution and could lead to alternative routes of adaptation where pathogens could either specialize on some host or evolve more generalist strategies. In a broader perspective, we believe that a better understanding of the spatial dynamics of pathogens requires detailed studies of the interplay between demography, stochasticity, and evolution occurring at the front line of epidemics.

Acknowledgments

We thank S. Lion for fruitful discussions. Useful comments on both the main text and the Supporting Information were supplied by A. E. Jan Engelstaedter, A. Perkins, and an anonymous referee. The work was funded by the CNRS, the ANR grant for the project MODEVOL: ANR-13-JS01-0009 to GR and the ERC Starting Grant 243054 EVOLEPID to SG. Our numerical analyses largely benefited from the Montpellier Bioinformatics Biodiversity computing cluster platform. SG and GR performed the modeling work, QG conducted the mathematical and numerical analysis. QG and SG wrote the first draft of the manuscript, and all authors contributed substantially to revisions. The authors have no competing interests.

DATA ARCHIVING

The simulation code was written in C++. It is available at:
https://gitlab.com/virulence_evolution_at_the_front_line_of_spreading_epidemics/Virulence_Evolution_at_the_front_line_of_spreading_epidemics_IBM

LITERATURE CITED

Alfaro, M., J. Coville, and G. Raoul. 2013. Travelling waves in a nonlocal equation as a model for a population structured by a space variable and a phenotypic trait. Commun. Part. Diff. Eq. 38:2126–2154.

Alizon, S., A. Hurford, M. Mideo, and M. Van Baalen, 2009. Virulence evolution and the trade-off hypothesis: history, current state of affairs and the future. J. Evol. Biol. 22:245–259.

Berger, L., R. Speare, P. Daszak, D. Green, A. Cunningham, Louise Goggin, Ron Slocombe, Mark A. Ragan, Alex D. Hyatt, Keith R. McDonald, et al. 1998. Chytridiomycosis causes amphibian mortality associated with population declines in the rain forests of Australia and Central America. Proc. Natl. Acad. Sci. USA 95:9031–9036.

Berngruber, T., R. Froissart, M. Choisy, and S. Gandon. 2013. Evolution of virulence in emerging epidemics. PLoS Pathog. 9. DOI:10.1371/journal.ppat.1003209.

Berngruber, T., S. Lion, and S. Gandon. 2015. Spatial structure, transmission modes and the evolution of viral exploitation strategies. PLoS Pathog. 11. DOI:10.1371/journal.ppat.1004810.

Biek, R., C. Henderson, L. Waller, C. Rupprecht, and L. Real. 2007. A high-resolution genetic signature of demographic and spatial expansion in epizootic rabies virus. Proc. Natl. Acad. Sci. USA 104:7993–7998.

Bolker, B. M., A. Nanda, and D. Shah. 2010. Transient virulence of emerging pathogens. J. R. Soc. Interface 7:811–822.

Boni, M., J. Gog, V. Andreasen, and M. Feldman. 2006. Epidemic dynamics and antigenic evolution in a single season of influenza A. Proc. R. Soc. B 273:1307–1316.

Boot, M., and A. Sasaki. 1999. Small worlds and the evolution of virulence: infection occurs locally and at a distance. Proc. R. Soc. B 206:1933–1938.

Boots, M., P. Hudson, and A. Sasaki. 2004. Large shifts in pathogen virulence relate to host population structure. Science 303:842–844.

Brunet, E., and B. Derrida. 1997. Shift in the velocity of a front due to a cutoff. Phys. Rev. E Stat. Nonlin. Soft Matter Phys. 56:2597–2604.

Bull, J., and D. Ebert. 2008. Invasion thresholds and the evolution of nonequilibrium virulence. Evol. Appl. 1:172–182.

Bull, J. J. 2006. Optimality models of phage life history and parallels in disease evolution. J. Theor. Biol. 241:928–938.

Burton, O., B. Phillips, and J. Travis. 2010. Trade-offs and the evolution of life-histories during range expansions. Ecol. Lett. 13:1210–1220.

Crow, J., and M. Kimura. 1970. An introduction to population genetics theory. Harper & Row, New York.

Day, T., and S. Gandon. 2007. Applying population-genetic models in theoretical evolutionary epidemiology. Ecol. Lett. 10:876–888.

———. 2012. Evolutionary epidemiology of multilocus drug resistance. Evolution 66:1582–1587.

Day, T., and S. Proulx. 2004. A general theory for the evolutionary dynamics of virulence. Am. Nat. 163:E40–E63.

Eller, S., and S. Schreiber. 2012. Temporally variable dispersal and demography can accelerate the spread of invading species. Theor. Popul. Biol. 86:283–298.

Eshelman, C., R. Vouk, J. L. Stewart, E. Halsne, H. A. Lindsey, S. Schneider, M. Gualu, A. M. Dean, and B. Kerr. 2010. Unrestricted migration favours virulent pathogens in experimental metapopulations: evolutionary genetics of a rapacious life history. Philos. Trans. R. Soc. B 365:2503–2513.

Farrer, R., L. Weinert, J. Biebly, T. Garner, F. Balloux, F. Clare, J. Bosch, A. A. Cunningham, C. Weldon, L. H. du Preez, et al. 2011. Multiple emergence of genetically diverse amphibian-infected chytrids include a globalized hypervirulent recombinant lineage. Proc. Natl. Acad. Sci. USA 108:18732–18736.

Fisher, R. A. 1937. The rate of advance of advantageous genes. Ann. Eugen. 7:355–369.

Frank, S. 1996. Models of parasite virulence. Q. Rev. Biol. 71:37–78.

Gallet, R., S. Kannoly, and I. Wang. 2011. Effects of bacteriophage traits on plaque formation. BMC Microbiol. 11.

Gandon, S., and T. Day. 2009. Evolutionary epidemiology and the dynamics of adaptation. Evolution 63:826–838.

Gandon, S., M. Hochberg, R. Holt, and T. Day. 2013. What limits the evolutionary emergence of pathogens? Philos. Trans. R. Soc. Lond. B Biol. Sci. 368. DOI:10.1098/rstb.2012.0086.

Gog, J., and T. Grenfell. 2002. Dynamics and selection of many-strain pathogens. Proc. Natl. Acad. Sci. USA 99:17209–17214.

Grenfell, B., O. Blornstad, and J. Kappey. 2001. Travelling waves and spatial hierarchies in measles epidemics. Nature 414:716–723.

Hallatschek, O., and D. Nelson. 2007. Gene surfing in expanding populations. Theor. Popul. Biol. 73:158–170.

———. 2009. Life at the front of an expanding population. Evolution 64:193–206.

Haraguchi, Y., and A. Sasaki. 2000. The evolution of parasite virulence and transmission rate in a spatially structured population. J. Theor. Biol. 203:85–96.

Holmes, E. 2009. The evolution and emergence of RNA viruses. Oxford Univ. Press, Oxford, UK.

James, T., A. Litvintseva, R. Vilgalys, J. Morgan, J. Taylor, M. C. Fisher, L. Berger, C. Weldon, L. du Preez, and J. E. Longcore. 2009. Rapid global expansion of the fungal disease chytridiomycosis into declining and healthy amphibian populations. PLoS Pathog. 5. DOI:10.1371/journal.ppat.1000458.

Kelehear, C., G. Brown, and R. Shine. 2012. Rapid evolution of parasite life history traits on an expanding range-edge. Ecol. Lett. 15:329–337.

Kolmogorov, A. N., I. G. Petrovsky, and N. S. Piskunov. 1937. Étude de l'équation de la diffusion avec croissance de la quantité de matière et son application à un problème biologique. Bulletin de l'Université d'État de Moscou.

Kot, M., M. Lewis, and P. van den Driessche. 1996. Dispersal data and the spread of invading organisms. Ecology 77:2027–2042.

Lenski, R., and R. May. 1994. The evolution of virulence in parasites and pathogens: reconciliation between two competing hypotheses. J. Theor. Biol. 169:253–265.

Lion, S., and M. Boots. 2010. Are parasites "prudent" in space? Ecol. Lett. 13:1245–1255.

Lion, S., and S. Gandon. 2015. Evolution of spatially structured host-parasite interactions. J. Evol. Biol. 28:10–28.

MacArthur, R., and E. Wilson. 1967. The theory of island biogeography. Princeton Univ. Press, Princeton, New Jersey, USA.

Mondet, F., J. de Miranda, A. Kretzschmar, Y. Le Conte, and A. Mercer. 2014. On the front line: quantitative virus dynamics in honeybee (*Apis mellifera* l.) colonies along a new expansion front of the parasite *Varroa destructor*. PLoS Pathog. 10. DOI:10.1371/journal.ppat.1004323.

Mueller, C., L. Mytnik, and J. Quatsel. 2011. Effect of noise propagation in reaction-diffusion equations of KPP type. Invent. Math. 184:405–453.

Mundt, C., K. Sackett, L. Wallace, C. Cowger, and J. Dudley. 2009. Long distance dispersal and accelerating waves of diseases: empirical relationship. Am. Nat. 173:456–466.

Osnas, E. E., P. J. Hurtado, and P. Dobson. 2015. Evolution of pathogen virulence across space during an epidemic. Am. Nat. 185:332–342.

Peischl, S., I. Dupanloup, M. Kirkpatrick, and L. Excoffier. 2013. On the accumulation of deleterious mutations during range expansion. Mol. Ecol. 22:5927–5982.

Perkins, T. 2012. Evolutionarily labile species interactions and spatial spread of invasive species. Am. Nat. 179:E37–E54.

Perkins, T., B. Phillips, M. Baskett, and A. Hastings. 2013. Evolution of dispersal and life history interact to drive accelerating spread of an invasive species. Ecol. Lett. 16:1079–1087.

Phillips, B. 2009. The evolution of growth rates at an expanding edge. Biol. Lett. 5:802–804.

Phillips, B., and R. Puschendorf. 2013. Do pathogens become more virulent as they spread? Evidence from the amphibian declines in Central America. Proc. R. Soc. B 280. DOI:10.1098/rspb.2013.1290.

Pianka, E. 1970. On $r-$ and $k-$selection. Am. Nat. 102:592–597.

———. 1972. r and k selection or b and d selection? Am. Nat. 106:581–588.

Pybus, O., M. Suchard, P. Lemey, F. Bernardin, A. Rambaut, F. W. Crawford, R. R. Gray, N. Arinaminpathy, S. L. Stramer, M. P. Busch, et al. 2012. Unifying the spatial epidemiology and molecular evolution of emerging epidemics. Proc. Natl. Acad. Sci. USA 109:15066–15071.

Roychoudhury, P., N. Shrestha, V. R. Wiss, S. M. Krone. 2014. Fitness benefits of low infectivity in a spatially structured population of bacteriophages. Proc. R. Soc. B 281. DOI:10.1098/rspb.2013.2563.

Seo, G., and F. Lutscher. 2011. Spread rates under temporal variability: calculation and application to biological invasions. Math. Models Methods Appl. Sci. 21:2469–2489.

Shigesada, N., and K. Kawasaki. 1997. Biological invasions: theory and practice. Oxford Univ. Press, Oxford, UK.

Shine, R., G. Brown, and B. Phillips. 2011. An evolutionary process that assembles phenotypes through space rather than through time. Proc. Natl. Acad. Sci. USA 108:5708–5711.

Skellam, J. 1951. Random dispersal in theoretical populations. Biometrika 38:196–268.

Snyder, R. E. 2003. How demographic stochasticity can slow biological invasions. Ecology 84:1333–1339.

Velo-Antòn, G., D. Rodríguez, A. Savage, G. Parra-Olea, K. Lips, and K. R. Zamudio. 2012. Amphibian-killing fungus loses genetic diversity as it spreads across the new world. Biol. Conserv. 146:213–218.

Voyles, J., S. Young, L. Berger, C. Campbell, W. Voyles, A. Dinudom, D. Cook, R. Webb, R. A. Alford, L. F. Skerratt, R. Speare, et al. 2009. Pathogenesis of chytridiomycosis, a cause of catastrophic amphibian decline. Science 326:582–585.

Wei, W., and S. Krone. 2005. Spatial invasion by a mutant pathogen. J. Theor. Biol. 236:335–348.

Yin, J. 1991. A quantifiable phenotype of viral propagation. Biochem. Biophys. Res. Commun. 174:1009–1014.

———. 1993. Evolution of bacteriophage t7 in a growing plaque. J. Bacteriol. 175:1272–1277.

Associate Editor: J. Engelstaedter
Handling Editor: J. Conner

Supporting Information

Additional Supporting Information may be found in the online version of this article at the publisher's website:

Figure S1. Position of the front with respect to time.
Figure S2. Shape of the stationary solution for an SI scenario with host demography.
Figure S3. Shape of the stationary solution for a SIR scenario.
Figure S4. Instantaneous speed of the front of the epidemic across time.
Table S1. Quantities versus dimensions.